Solitons in weakly nonlocal media with cubic-quintic nonlinearity

Eduard N. Tsoy

Physical-Technical Institute of the Uzbek Academy of Sciences, Bodomzor Street 2-B, Tashkent-84, 100084 Uzbekistan

(Received 22 October 2010; published 27 December 2010)

The propagation of optical beams in weakly nonlocal media with cubic-quintic nonlinearity is studied. The exact solutions for bright and dark solitons are found. The general solutions are implicit, and they are expressed in terms of the elliptic integrals. In particular cases, the solutions are written explicitly in terms of the hyperbolic functions. The dependence of the beam parameters and the soliton shapes on the system parameters is analyzed. The role of nonlocality on the soliton stability is investigated.

DOI: 10.1103/PhysRevA.82.063829 PACS number(s): 42.65.Tg, 42.65.Jx, 05.45.Yv

I. INTRODUCTION

A strong optical beam propagating in a nonlinear medium induces a variation Δn of the refractive index. In Kerr-type media, this variation depends on the local intensity of the beam. However, in general, Δn should be considered as a nonlocal function of intensity. In this case, Δn is written as a convolution of the medium response function and the intensity-dependent function.

Usually, nonlocality originates from other processes that accompany the beam propagation, such as heat transfer in media with thermal nonlinearity [1–3], diffusion of particles [4–7], and a change of molecule orientation [8–11]. Nonlocal interaction is also important in the dynamics of ultracold atomic gases [12–15].

Recent advances in the study of nonlocal media in optics are related mainly to research on the beam propagation in photorefractive media [4–7] and in liquid crystals [8–11]. The soliton dynamics and interaction in these media have been investigated theoretically and experimentally.

The propagation of a beam in nonlinear media is described in the paraxial approximation by the following equation [16]:

$$i\,\partial_z\psi + \frac{1}{2\beta_0}\,\partial_x^2\psi + k_0\Delta n(I)\,\psi = 0\,, \tag{1}$$

where $\psi(x,z)$ is the envelope of the electromagnetic field, x and z are the transverse and longitudinal coordinates, respectively, $\beta_0 = k_0 n_0$ is the propagation constant, $k_0 = 2\pi/\lambda_0$, n_0 is the linear index, and λ_0 is the laser wavelength. We will consider Eq. (1) in dimensionless form, taking $\beta_0 = k_0 = 1$. For nonlocal nonlinear media, $\Delta n(I)$ is represented as [17,18]

$$\Delta n(I) = \int_{-\infty}^{\infty} R(x'-x) f(I(x',z)) dx'\,, \tag{2}$$

where $f(I)$ is the intensity-dependent function and $I(x,z) \equiv |\psi(x,z)|^2$. The medium response function $R(x)$ is a real symmetric function, which is normalized to unity.

For media with cubic nonlinearity, $f(I)$ is proportional to I. In this work, we include the next term in the Taylor expansion, taking $f(I) = \gamma I + \delta I^2$. Also, we consider a case of *weak* nonlocality. This assumption is valid when the size of the intensity distribution $I(x,z)$ in the transverse direction x is much larger than the spatial width of $R(x)$ (see, e.g., Ref. [17]). Then $I(x',z)$ in Eq. (2) can be expanded around $x' = x$, so that

$$\Delta n(I) = \gamma I + \delta I^2 + \mu\,\partial_x^2 I, \tag{3}$$

where $\mu = \frac{1}{2}\int_{-\infty}^{\infty} x^2 R(x) dx$ characterizes the degree of nonlocality. In the derivation of Eq. (3), we ignore higher-order terms, such as $\sim\partial_x^2 I^2$.

Equation (1), together with Eq. (3), results in the cubic-quintic nonlinear Schrödinger (NLS) equation with weak nonlocality:

$$i\,\partial_z\psi + \tfrac{1}{2}\partial_x^2\psi + \gamma|\psi|^2\psi + \delta|\psi|^4\psi + \mu\,\psi\,\partial_x^2|\psi|^2 = 0. \tag{4}$$

When $R(x)$ does not change sign over x, the signs of γ and μ are the same. Here we consider a case in which the signs of γ and μ are not related to each other. Equation (4) has a general character, and it is valid for other nonlocal systems. For example, in the physics of ultracold atoms, Eq. (4) describes the dynamics of Tonks-Girardo gas in a weakly nonlocal limit [14].

The aim of the present work is to present exact analytical solutions for stationary bright and dark solitons in nonlocal nonlinear media. For weakly nonlocal media with cubic nonlinearity, the soliton solutions in an implicit form have been found in Ref. [17]. Our work provides an extension of these results to media with cubic-quintic nonlinearity. In general, the solutions found are in implicit form. However, we also find the conditions under which the solutions are expressed explicitly in terms of hyperbolic functions. We also analyze, using the invariants of Eq. (4), the stability of solitons.

II. BRIGHT SOLITONS

We search for solutions of Eq. (4) in the following form:

$$\psi(x,z) = \rho(\xi)\exp[i\phi(\xi)]\,\exp(ikz), \tag{5}$$

where $\xi = x - vz$, v is the soliton transverse velocity, and $k > 0$ is the propagation constant. By substituting Eq. (5) into Eq. (4) and separating the real and imaginary parts, we obtain equations for the soliton shape $\rho(\xi)$ and phase $\phi(\xi)$:

$$\frac{1}{2}\rho'' + \left(v\phi' - k - \frac{1}{2}\phi'^2\right)\rho + \gamma\rho^3 + \delta\rho^5 + \mu(\rho^2)''\rho = 0,$$

$$\frac{1}{2}\rho\phi'' + (\phi' - v)\rho' = 0, \tag{6}$$

where the prime denotes the derivative on ξ. It follows from the second of Eqs. (6) that $\rho^2(\phi' - v) = 0$. Therefore, $\phi(\xi) = v\xi + \phi_0$, where ϕ_0 is the initial phase. Then the first of Eqs. (6) can be integrated once. The integration constant equals zero, because ρ and all its derivatives vanish at $\xi \to \infty$. Now we introduce an auxiliary parameter ρ_a, such that $\rho' = 0$, when $\rho = \rho_a$. Parameter ρ_a is used later in a definition of the soliton amplitude. Then

$$k = v^2/2 + \gamma\rho_a^2/2 + \delta\rho_a^4/3, \tag{7}$$

and the equation for ρ is written as

$$\rho'^2 = \rho^2\left(\rho_a^2 - \rho^2\right)\frac{\gamma + 2\delta\left(\rho_a^2 + \rho^2\right)/3}{1 + 4\mu\rho^2} \equiv -U(\rho). \tag{8}$$

Relation (7) for the propagation constant is the same as that for cubic-quintic media with local interaction.

For the existence of bright solitons, the function $U(\rho)$ in Eq. (8) should satisfy the following conditions: (i) $\rho = 0$ is the root and the maximum point of $U(\rho)$ (i.e., $dU/d\rho = 0$ and $d^2U/d\rho^2 < 0$ at $\rho = 0$), and (ii) there exists a root $\rho = \rho_m$ of $U(\rho)$, such that $U(\rho) < 0$ for $0 < \rho < \rho_m$. These conditions define the amplitude thresholds for the existence of bright solitons. For $\gamma > 0$, solitons exist if

$$\begin{gathered}\delta > 0,\ \mu > 0,\ \text{and any } \rho_a,\\ \delta > 0,\ \mu < 0,\ \text{and } \rho_a^2 < -1/(4\mu),\\ \delta < 0,\ \mu > 0,\ \text{and } \rho_a^2 < |3\gamma/(2\delta)| \equiv \rho_c^2,\\ \delta < 0,\ \mu < 0,\ \text{and } \rho_a^2 < \rho_c^2\\ \text{and } \rho_m^2 < -1/(4\mu).\end{gathered} \tag{9}$$

For $\gamma > 0$, the soliton amplitude ρ_m is defined as

$$\rho_m = \begin{cases} \rho_a & \text{for } \delta > 0,\\ \min\left[\rho_a, \sqrt{\frac{-3\gamma}{2\delta} - \rho_a^2}\right] & \text{for } \delta < 0. \end{cases} \tag{10}$$

For $\gamma < 0$, solitons exist if

$$\begin{gathered}\delta > 0,\ \mu > 0,\ \text{and } \rho_a^2 > \rho_c^2,\\ \delta > 0,\ \mu < 0,\ \text{and } -1/(4\mu) > \rho_a^2 > \rho_c^2.\end{gathered} \tag{11}$$

In this case $\rho_m = \rho_a$. The existence of bright solitons for the defocusing Kerr coefficient, $\gamma < 0$, is not surprising, because such solitons are possible in *local* cubic-quintic media [see Ref. [19] and Eq. (18)]. However, in local media, such solutions are unstable. We will demonstrate that nonlocality ($\mu > 0$) can stabilize high-amplitude bright solitons in media with $\gamma < 0$.

As pointed out in Eq. (9), for $\delta < 0$ and $\mu > 0$, the parameter ρ_a can be varied from zero to ρ_c. Actually, one can consider values of ρ_a in the range $[0, \rho_c/\sqrt{2}]$ only. In this case, the soliton amplitude is $\rho_m = \rho_a$. One can show that a solution of Eq. (8) with $\rho_a = \rho_{a,1} \in [0, \rho_c/\sqrt{2}]$ is the same as a solution with $\rho_a = \rho_{a,2} \in [\rho_c/\sqrt{2}, \rho_c]$, provided that $\rho_{a,1}^2 + \rho_{a,2}^2 = \rho_c^2$. This is because the right-hand side of Eq. (8) is identical for $\rho_a = \rho_{a,1}$ and for $\rho_a = \rho_{a,2}$ [see also Eq. (10)]. A similar argument is valid when $\delta < 0$ and $\mu < 0$. Here one can consider that ρ_a varies from zero to $\min[\rho_c/\sqrt{2}, \sqrt{-1/(4\mu)}]$. We consider the whole region of ρ_a for completeness.

Equation (8) can be integrated, giving implicit solutions for bright solitons. To simplify notation, we introduce two parameters a and b:

$$a = -\frac{3\gamma}{2\delta} - y_a, \quad b = -\frac{1}{4\mu}, \tag{12}$$

where $y_a \equiv \rho_a^2$. For $\delta > 0$, $\mu > 0$, and $y_a > 0 > a > b$, the solution is written as follows:

$$\begin{aligned}\pm\xi = \frac{1}{2}\sqrt{\frac{3}{2\delta\mu}}\,\frac{1}{y_a\sqrt{y_a - b}}\,&[\Pi(\lambda_1, (y_a - a)/y_a, q_1)\\ &+ 4\mu y_a F(\lambda_1, q_1)],\\ \lambda_1 = \sin^{-1}\sqrt{\frac{y_a - y}{y_a - a}}, &\quad q_1 = \sqrt{\frac{y_a - a}{y_a - b}},\end{aligned} \tag{13}$$

where $y(\xi) \equiv \rho^2(\xi)$. Functions $F(\lambda, q)$ and $\Pi(\lambda, m, q)$ are the elliptic integrals of the first and third kinds, respectively [20] (see the Appendix). If $\delta > 0$, $\mu > 0$, and $y_a > 0 > b > a$, then the solution is obtained from Eq. (13) by using the transformation $a \leftrightarrow b$. In both cases the soliton peak intensity is $y_m \equiv \rho_m^2 = y_a$, as a nearest-to-zero positive root of $U(\rho)$.

For $\delta > 0$ and $\mu < 0$, the solution is

$$\begin{aligned}\pm\xi = \frac{1}{2}\sqrt{\frac{3}{2|\delta\mu|}}\,\frac{1}{by_a\sqrt{b - a}}\,&\left[(b - y_a)\,\Pi\left(\lambda_2, q_2^2 b/y_a, q_2\right)\right.\\ &\left.+ (1 + 4\mu b)\,y_a\,F(\lambda_2, q_2)\right],\\ \lambda_2 = \sin^{-1}\sqrt{\frac{(b - a)(y_a - y)}{(y_a - a)(b - y)}}, &\quad q_2 = \sqrt{\frac{y_a - a}{b - a}},\end{aligned} \tag{14}$$

where $b > y_a > 0 > a$. For $\delta < 0$, $\mu > 0$, and $a > y_a > 0 > b$ the solution with $y_m = y_a$ is obtained from Eq. (14) by using the transformation $a \leftrightarrow b$. When $y_a > a > 0 > b$, the solution with $y_m = a$ is obtained from Eq. (14) by using the transformations $a \to b$, $b \to y_a$, and $y_a \to a$.

For $\delta < 0$, $\mu < 0$, and $b > a > y_a > 0$, the solution has the form

$$\begin{aligned}\pm\xi = \frac{1}{2}\sqrt{\frac{3}{2|\delta\mu|}}\,\frac{1}{ay_a\sqrt{b - y_a}}\,&[(a - y_a)\Pi(\lambda_3, a/y_a, q_3)\\ &+ (1 + 4\mu a)\,y_a\,F(\lambda_3, q_3)],\\ \lambda_3 = \sin^{-1}\sqrt{\frac{y_a - y}{a - y}}, &\quad q_3 = \sqrt{\frac{b - a}{b - y_a}}.\end{aligned} \tag{15}$$

For $\delta < 0$ and $\mu < 0$, three other cases should be considered. In all of these cases, the solution is obtained from Eq. (15) with the corresponding transformations of the parameters, as follows:

$$\begin{gathered}a > b > y_a > 0, \quad \text{then} \quad a \leftrightarrow b,\\ b > y_a > a > 0, \quad \text{then} \quad a \leftrightarrow y_a,\\ y_a > b > a > 0, \quad \text{then} \quad a \to b, b \to y_a, y_a \to a.\end{gathered} \tag{16}$$

The solutions (13)–(15) are valid for any sign of γ, provided that the corresponding conditions [see Eqs. (9) and (11)] for ρ_a and ρ_m are fulfilled.

For a particular value of the soliton amplitude, the fraction in Eq. (8) can be reduced to a constant that depends only

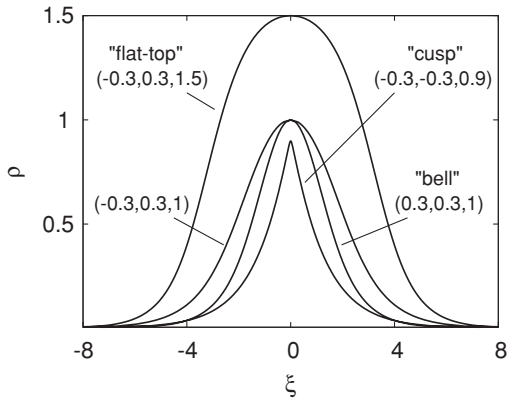

FIG. 1. Examples of different soliton shapes. Lines are labeled by values of (δ,μ,ρ_m).

on the system parameters. Then the solution of Eq. (8) has a hyperbolic secant form, which is similar to the standard NLS equation:

$$\rho(\xi)=\rho_m\,\mathrm{sech}\left[\frac{\rho_m}{2}\sqrt{\frac{2\delta}{3\mu}}\,(\xi-\xi_0)\right],$$
$$\rho_m^2=\frac{1}{4\mu}-\frac{3\gamma}{2\delta}>0,\quad \delta\mu>0. \tag{17}$$

For $\gamma>0$, if $\delta>0$ and $\mu>0$, this solution exists when $\delta>6\gamma\mu$, while if $\delta<0$ and $\mu<0$, it exists when $3\gamma\mu>\delta>6\gamma\mu$. For $\gamma<0$, $\delta>0$, and $\mu>0$, solution (17) is valid for any δ and μ.

Equation (8) for $\mu=0$ corresponds to a local cubic-quintic medium. In this case, Eq. (8) has an explicit solution [19]:

$$\rho(\xi)=\frac{2\sqrt{k}}{\sqrt{\gamma+\sqrt{\gamma^2+16\delta k/3}\,\cosh(2\sqrt{2k}\,\xi)}}, \tag{18}$$

where k is given by Eq. (7). This solution is valid for any sign of γ. For $\gamma>0$ and $\delta<0$, the soliton form tends to a flat-top profile, when $k\to-3\gamma^2/(16\delta)$.

Examples of the soliton solutions (13)–(15) are presented in Fig. 1. The soliton width, as well as the soliton shape, depend on the system parameters and the amplitude ρ_m. Solitons in nonlocal media can have a cusp shape, a bell shape, or a flat-top profile.

Figure 2 shows the dependence of the inverse of the soliton width [full width at half maximum (FWHM) of the intensity] on the soliton amplitude for $\gamma>0$. For fixed ρ_m and $\delta>0$, solitons become wider for larger $\mu>0$ [see Fig. 2(a)]. This means that more power is necessary to create a soliton in media with larger μ. This fact can be explained by the following argument. Qualitatively, one can say that nonlocality (nl) induces an additional potential $V_{\rm nl}=\mu\partial_x^2|\psi(x,z)|^2$. For $\mu<0$ ($\mu>0$), the nonlocality potential is positive (negative) near the soliton peak and negative (positive) near the soliton edges. This can be interpreted to mean that for $\mu<0$ ($\mu>0$), nonlocality increases self-focusing (self-defocusing) properties near the beam core and self-defocusing (self-focusing) properties near the beam edges.

When $\delta<0$ or $\mu<0$, the soliton amplitude is bounded by the threshold amplitude [see Eqs. (9) and (10)]. Moreover, as

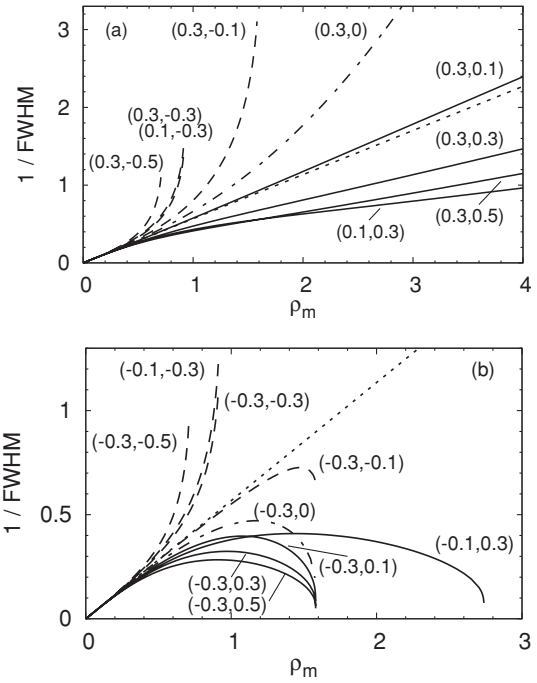

FIG. 2. Inverse of soliton FWHM as a function of the amplitude ρ_m for $\gamma=1$, and for (a) $\delta>0$ and (b) $\delta<0$. Lines are labeled by values of (δ,μ). Solid (dashed) lines are for $\mu>0$ ($\mu<0$). The dotted (dash-dotted) line corresponds to the standard (cubic-quintic) NLS soliton, $\delta=\mu=0$ ($\mu=0$).

we will show later, for $\mu<0$, the solitons with amplitude close to the threshold become unstable. This is because of additional self-focusing near the soliton center due to nonlocality.

As seen from Fig. 2(b), for $\delta<0$ there exist two types of beams with the same width. These beams have different amplitudes and, therefore, different total powers. This property, which is peculiar to the local cubic-quintic NLS equation [21], remains in the weakly nonlocal media as well.

Figure 3 shows the relation between the soliton parameters for $\gamma<0$. For moderate $\delta>0$ and $\mu>0$, the soliton width is larger than that of the standard NLS soliton of the same amplitude. An increase of the nonlocality parameter μ makes the solitons wider. As will be demonstrated later, only high-amplitude solitons are stable for $\gamma<0$, $\delta>0$, and $\mu>0$. For $\gamma<0$, $\delta>0$, and $\mu<0$, solitons with any amplitude are unstable; therefore, their characteristics are not shown in Fig. 3.

To analyze the beam shape, we introduce the shape parameter $s(\alpha)$, which is the ratio of the width of the intensity distribution at level αy_m to the FWHM. We take $\alpha=0.9$ in the forthcoming analysis. As a reference, we mention that $s(0.9)=0.152$ for a cusp shape of $\rho(x)\sim\exp(-|x/w|)$, $s(0.9)=0.175$ for a triangular shape of $\rho(x)$, $s(0.9)=0.2$ for a triangular shape of $\rho^2(x)$, $s(0.9)=0.372$ for a $\rho(x)\sim\mathrm{sech}(x/w)$ shape, $s(0.9)=0.390$ for a $\rho(x)\sim\exp[-x^2/(2w^2)]$ shape, $s(0.9)=0.624$ for a $\rho(x)\sim\exp[-x^4/(2w^4)$ shape, and $s=1$ for a rectangular box, where w is the width parameter. For a super-Gaussian shape of $\rho(x)\sim\exp[-x^{2n}/(2w^{2n})]$, where $n>1$ is an integer, the larger n is, the more the soliton shape approaches the flat-top profile. Correspondingly, the parameter

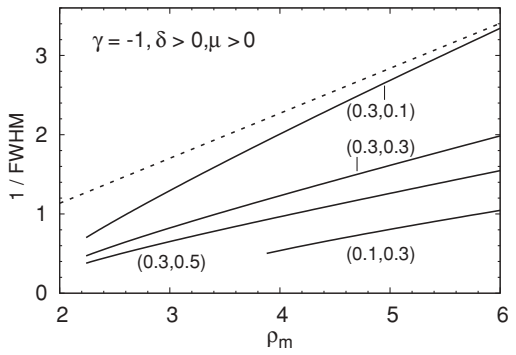

FIG. 3. Same as in Fig. 2, but for $\gamma = -1$, $\delta > 0$, and $\mu > 0$.

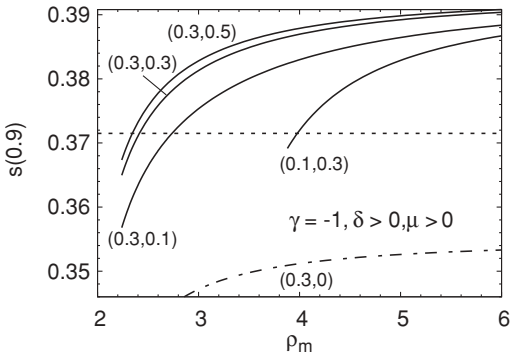

FIG. 5. Same as in Fig. 4, but for $\gamma = -1$, $\delta > 0$, and $\mu > 0$.

s increases with n. Therefore, we see that s can be used to distinguish effectively between cusp, bell, and flat-top profiles.

The dependence of the shape parameter on the soliton amplitude presented in Figs. 4 and 5 for the different system parameters is summarized as follows. For $\gamma > 0$ (see Fig. 4) and

(i) for $\delta > 0$ and $\mu > 0$: $s(0.9)$ depends weakly on δ, μ, and ρ_m, varying near the NLS soliton value.

(ii) for $\delta > 0$ and $\mu < 0$: The dependence of $s(0.9)$ on ρ_m changes sharply, when $|\mu|$ increases. The beam profile tends to the cusp shape, when $\rho_m \to b^{1/2}$.

(iii) for $\delta < 0$ and $\mu > 0$: The dependence of $s(0.9)$ on ρ_m, which is close to that of the local cubic-quintic NLS soliton, changes slightly by varying μ for fixed δ. The beam tends to the flat-top shape, when $\rho_m \to \rho_c/\sqrt{2}$.

(iv) for $\delta < 0$ and $\mu < 0$: The dependence of $s(0.9)$ on ρ_m changes sharply, when $|\mu|$ deviates slightly from zero; see, for example, curves for $\mu = -0.1$ and for $\mu = -0.3$. The beam profile tends to the cusp shape, when ρ_m approaches to the maximum of allowed values.

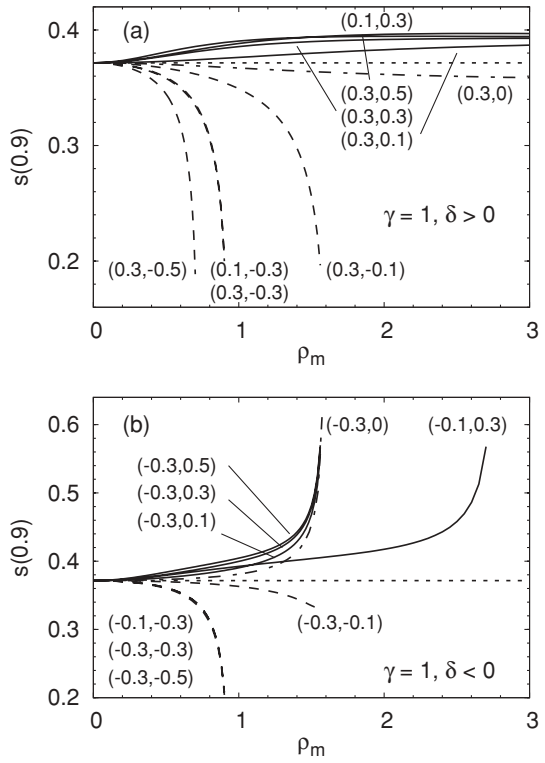

FIG. 4. Soliton shape parameter $s(0.9)$ as a function of the amplitude ρ_m for $\gamma = 1$, and for (a) $\delta > 0$ and (b) $\delta < 0$. Lines are labeled by values of (δ, μ). Solid (dashed) lines are for $\mu > 0$ ($\mu < 0$). The dotted (dash-dotted) line corresponds to the standard (qubic-quintic) NLS soliton, $\delta = \mu = 0$ ($\mu = 0$).

For the analysis of the soliton stability, we use the invariant of Eq. (4), which is the beam power:

$$P = \int_{-\infty}^{\infty} |\psi(x,z)|^2 dx. \tag{19}$$

For a solution in the form of Eq. (5), P can be calculated by using Eq. (8). According to the Vakhitov-Kolokolov condition [16], the soliton stability is determined by the dependence of P on the propagation constant k. The soliton is stable if $dP/dk > 0$ and unstable otherwise.

The beam power of the solutions (13)–(15) can be found explicitly. For $\delta > 0$, $\mu > 0$, and $y_a > 0 > a > b$ one has

$$P = 2\sqrt{\frac{6\mu}{\delta}}\,\sqrt{y_a - b}\,E(\lambda_{10}, q_1), \tag{20}$$

where $\lambda_{10} = \lambda_1(y = 0)$ and $E(\lambda, q)$ is the elliptic integral of the second kind (see the Appendix).

For $\delta > 0$, $\mu > 0$, and $y_a > 0 > b > a$, P is found as

$$P = \sqrt{\frac{3}{2\delta\mu}}\,\frac{1}{\sqrt{y_a - a}}\,[(1 + 4\mu a)F(\bar{\lambda}_{10}, \bar{q}_1) + 4\mu(y_a - a)\,E(\bar{\lambda}_{10}, \bar{q}_1)], \tag{21}$$

where

$$\bar{\lambda}_{10} = \sin^{-1}\sqrt{\frac{y_a}{y_a - b}}, \quad \bar{q}_1 = \sqrt{\frac{y_a - b}{y_a - a}}. \tag{22}$$

As expected, Eq. (21) is reduced to Eq. (20) by using the transformation $a \leftrightarrow b$, since the expression in brackets in front of F vanishes in this case.

For $\delta > 0$, $\mu < 0$, and $b > y_a > 0 > a$,

$$P = 2\sqrt{\frac{6|\mu|}{\delta}}\,\frac{(b - y_a)}{\sqrt{b - a}}\,\Pi\left(\lambda_{20}, q_2^2, q_2\right), \tag{23}$$

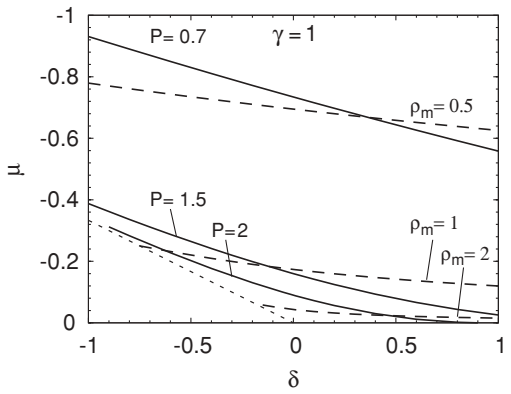

FIG. 6. Diagram of the stability of bright solitons for $\gamma = 1$. Solid (dashed) lines are the threshold isolines for constant values of P (of ρ_m). For given values of δ and μ, solitons with the power (amplitude) smaller than the label value are stable. The dotted line marks the border of the soliton existence region.

where $\lambda_{20} = \lambda_2(y = 0)$.

For $\delta < 0$, $\mu > 0$, and $a > y_a > 0 > b$,

$$P = \sqrt{\frac{3}{2|\delta|\mu}}\,\frac{1}{\sqrt{a-b}}\left[(1+4\mu a)F(\bar{\lambda}_{20},\bar{q}_2) + 4\,\mu(y_a-a)\,\Pi\left(\bar{\lambda}_{20},\bar{q}_2^2,\bar{q}_2\right)\right], \tag{24}$$

where

$$\bar{\lambda}_{20} = \sin^{-1}\sqrt{\frac{(a-b)y_a}{(y_a-b)a}}, \quad \bar{q}_2 = \sqrt{\frac{y_a-b}{a-b}}. \tag{25}$$

For $\delta < 0$, $\mu > 0$, and $y_a > a > 0 > b$, P is obtained from Eqs. (24) and (25) by using $a \leftrightarrow y_a$.

For $\delta < 0$, $\mu < 0$, and $b > a > y_a > 0$,

$$P = \sqrt{\frac{3}{2|\delta\mu|}}\,\frac{1}{\sqrt{b-y_a}}\,[(1+4\mu y_a)F(\lambda_{30},q_3) + 4\,\mu(b-y_a)\,E(\lambda_{30},q_3) - 4\mu\sqrt{by_a(b-y_a)/a}], \tag{26}$$

where $\lambda_{30} = \lambda_3(y = 0)$. For different relations between a, b, and y_a, P is obtained from Eq. (26) by using the corresponding transformation from Eq. (16). As a reference, we mention that $P = 4\rho_m\sqrt{3\mu/(2\delta)}$ for the solution (17).

Equations (20)–(26) and (7) provide the dependence, parametrized by ρ_a, of the power on the propagation constant. First we analyze the soliton stability at $\gamma > 0$. The function $P(k)$ increases monotonically for $\mu > 0$; therefore, solitons are stable in this region of the parameters. For $\mu < 0$, $P(k)$ might have a maximum. The maximum defines a threshold (th) value of $k_{\rm th}$, above which solitons are unstable ($dP/dk < 0$). Since ρ_m depends monotonically on k (at least when $\rho_a < \rho_c/\sqrt{2}$), the threshold $k_{\rm th}$ also defines the threshold amplitude $\rho_{m,\rm th}$. Isolines of the threshold power $P_{\rm th} \equiv P(k_{\rm th})$ and amplitude in the (δ,μ) plane are shown in Fig. 6. As seen from the figure, only low-intensity (amplitude) solitons are stable for large values of $|\mu|$.

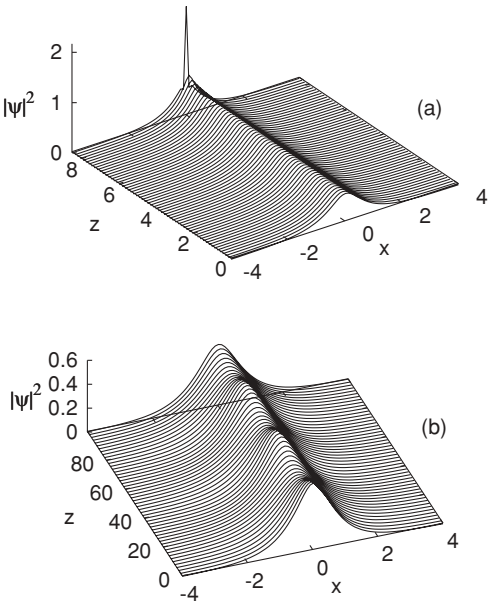

FIG. 7. Dynamics of bright solitons for $\gamma = -1$, $\delta = 0.3$, $\mu = -0.3$, and $\rho_{m,0} = 0.75$. The thresholds for these parameters are $P_{\rm th} = 1.008$ and $\rho_{m,\rm th} = 0.735$. (a) A soliton collapses, when $\varepsilon = 0.005$ and $P_0 = 1.013$. (b) The soliton oscillates, when $\varepsilon = -0.005$ and $P_0 = 1.003$.

A particular manner of the instability development depends on the system parameters and initial conditions. As an initial condition we take

$$\psi(x,0) \equiv \psi_0(x) = [1 + \varepsilon r(x)]\psi_{\rm ex}(x,0), \tag{27}$$

where ε is the perturbation parameter, $r(x) \in [0,1]$ is the random function with uniform distribution, and $\psi_{\rm ex}(x,0)$ is one of the exact (ex) solutions given by Eq. (5) and Eqs. (13)–(17). A typical scenario of the dynamics observed in the numerical simulations of Eq. (4) for $\gamma > 0$ is the following. When the initial power P_0 is larger than the threshold power $P_{\rm th}$, $P_0 > P_{\rm th}$, the soliton collapses [i.e. the soliton amplitude increases sharply, while the soliton width decreases; see Fig. 7(a)]. When $P_0 < P_{\rm th}$ and $\rho_{m,0} < \rho_{m,\rm th}$, where $\rho_{m,0}$ is the initial soliton amplitude, the soliton oscillates close to the initial profile. When $P_0 < P_{\rm th}$ and $\rho_{m,0} > \rho_{m,\rm th}$, then, depending on ϵ, the soliton either collapses (when $\varepsilon > \varepsilon_{\rm th}$, where $\varepsilon_{\rm th} > 0$ is a threshold value), or oscillates (when $\varepsilon < \varepsilon_{\rm th}$) near a stationary profile [see Fig. 7(b)]. That profile has the amplitude smaller than $\rho_{m,\rm th}$. We recall that $P_{\rm th}$ corresponds to a maximum of the dependence $P(\rho_m)$ [as well as of $P(k)$]. Therefore, the unstable soliton with $\rho_{m,0} > \rho_{m,\rm th}$ and $P_0 < P_{\rm th}$ is switched to the state on the stable branch with $\rho_m < \rho_{m,\rm th}$.

The results of the soliton stability at $\gamma < 0$ are summarized in Fig. 8. For given $\delta > 0$ and $\mu > 0$, the dependence $P(k)$ has a minimum at $k = k_{\rm th}$. This minimum defines the threshold values of the power $P_{\rm th}$ and amplitude $\rho_{m,\rm th}$. Low-amplitude solitons with $\rho_m < \rho_{m,\rm th}$ correspond to the unstable branch, where $dP/dk < 0$, while high-amplitude solitons with $\rho_m > \rho_{m,\rm th}$ are stable since $dP/dk > 0$. In local cubic-quintic media with $\gamma < 0$ and $\delta > 0$, stable solitons do not exist. Thus, nonlocal effects can stabilize high-amplitude solitons in media with $\gamma < 0$. Here, an interplay of cubic

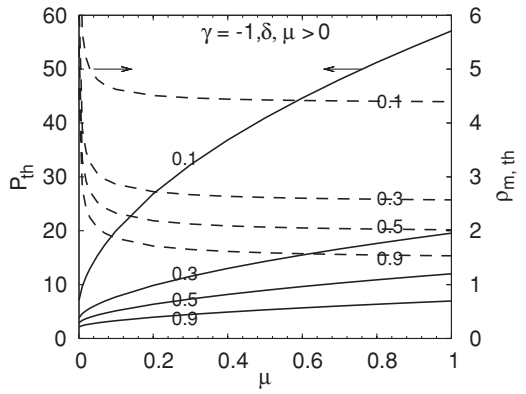

FIG. 8. Diagram of the stability of bright solitons for $\gamma = -1$. Solid lines correspond to $P_{\rm th}(\mu)$ for a given δ, while dashed lines correspond to $\rho_{m,\rm th}(\mu)$. Lines are labeled by δ values. Solitons with power (amplitudes) larger than the threshold are stable.

self-defocusing, quintic self-focusing, and space-dependent focusing (defocusing) due to nonlocality results in effective nonlinearity that balances diffraction.

Numerical simulations of Eq. (4) for $\gamma < 0$ with initial condition (27) reveal the following dynamics of the perturbed soliton. First, consider $\delta > 0$ and $\mu > 0$. If $P_0 < P_{\rm th}$, the soliton spreads (see Fig. 9). When $P_0 > P_{\rm th}$ and $\rho_{m,0} > \rho_{m,\rm th}$, the soliton oscillates near the initial profile. When $P_0 > P_{\rm th}$ and $\rho_{m,0} < \rho_{m,\rm th}$, then, depending on value of ε, the soliton either spreads or oscillates near the stable profile with $\rho_m > \rho_{m,\rm th}$. For $\delta > 0$ and $\mu < 0$, solitons are always unstable. Depending on initial conditions, solitons either collapse or spread for this set of the parameters.

III. DARK SOLITONS

A dark soliton corresponds to a dip on a constant background [16]. We search for the dark soliton solutions, also in the form of Eq. (5). Now, the second of Eqs. (6) results in the following relation for the soliton phase:

$$\phi' = v(1 - y_b/y), \tag{28}$$

where $y(\xi) = \rho^2(\xi)$, $y_b = \rho_b^2$, and ρ_b is the background amplitude, such that $\rho \to \rho_b$ at $\xi \to \pm\infty$. The first of Eqs. (6) and the boundary conditions at $\xi \to \pm\infty$ give the relation for the propagation constant

$$k = \gamma y_b + \delta y_b^2. \tag{29}$$

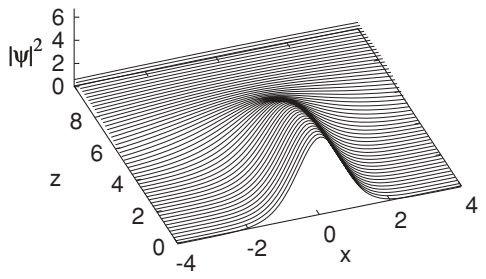

FIG. 9. Spreading of a soliton for $\gamma = -1$, $\delta = 0.3$, and $\mu = 0.3$. Initial conditions are $\rho_{m,0} = 2.6$, $P_0 = 11.51$, and $\varepsilon = -0.005$. The thresholds are $P_{\rm th} = 11.54$ and $\rho_{m,\rm th} = 2.67$.

Similarly to Sec. II, we introduce an auxiliary parameter ρ_a (or $y_a = \rho_a^2$), such that $\rho' = 0$, when $\rho = \rho_a$. Then

$$v^2 = -y_a^2[\gamma + 2\delta(2y_b + y_a)/3], \tag{30}$$

and the equation for $y(\xi)$ has the form

$$y'^2 = -4(y_b - y)^2(y - y_a) \times \frac{[\gamma + 2\delta(y + 2y_b + y_a)/3]}{1 + 4\mu y} \equiv -U_d(y). \tag{31}$$

For the existence of dark solitons, the following conditions should be satisfied: (i) $y = y_b$ is the root and the maximum point of $U_d(y)$, (ii) $U_d(y) < 0$ for $y_m \leqslant y \leqslant y_b$, where y_m is the value at the minimum of $y(\xi)$, and (iii) v^2 in Eq. (30) is non-negative. These conditions define threshold values of y_b and y_a for the existence of dark solitons. Similarly to Sec. II, we introduce two parameters:

$$a = -\frac{3\gamma}{2\delta} - 2y_b - y_a, \quad b = -\frac{1}{4\mu}. \tag{32}$$

Then, for $\gamma < 0$ we have the following conditions for the existence of dark solitons

$$\begin{aligned}
&\delta > 0 \text{ and } \mu > 0: \text{ if } a > y_b > y_a \Rightarrow\ 3y_b + y_a < y_c,\\
&\quad \text{if } y_a > y_b > a \Rightarrow\ 3y_b + y_a > y_c > 2y_b + y_a,\\
&\delta > 0 \text{ and } \mu < 0: \text{ if } a > y_b > y_a\\
&\qquad \Rightarrow\ 3y_b + y_a < y_c \text{ and } y_b < b,\\
&\quad \text{if } y_b > y_a > a \Rightarrow\ 2y_b + y_a < y_c,\\
&\qquad y_b + y_a > y_c/2 \text{ and } y_a > b,\\
&\quad \text{if } y_b > a > y_a \Rightarrow\ 3y_b + y_a > y_c,\\
&\qquad y_b + y_a < y_c/2 \text{ and } a > b,\\
&\quad \text{if } y_a > y_b > a \Rightarrow\ 3y_b + y_a > y_c > 2y_b + y_a\\
&\qquad \text{and } y_b < b,\\
&\qquad \delta < 0 \text{ and } \mu > 0: \text{ any } y_a < y_b,\\
&\qquad \delta < 0 \text{ and } \mu < 0: \ b > y_b > y_a.
\end{aligned} \tag{33}$$

For $\gamma > 0$, the conditions are

$$\begin{aligned}
&\delta < 0 \text{ and } \mu > 0: \ y_b > y_a \text{ and } 2y_b + y_a > y_c,\\
&\delta < 0 \text{ and } \mu < 0: \ b > y_b > y_a \text{ and } 2y_b + y_a > y_c.
\end{aligned} \tag{34}$$

No dark solitons exist for $\gamma > 0$ and $\delta > 0$. The minimum intensity y_m of the dark soliton is found as nearest to y_b and smaller than that root of $U(y)$. We note that, in cubic-quintic nonlocal media, dark solitons exist for any sign of cubic nonlinearity γ as well.

Here we represent only an explicit solution that is realized when the fraction in Eq. (30) is reduced to a constant. This is possible when the following condition is satisfied:

$$2y_b + y_m = -\frac{3\gamma}{2\delta} + \frac{1}{4\mu} > 0, \tag{35}$$

where we take $y_a = y_m$. For these values of the parameters,

the dark soliton solution has the form

$$\rho(\xi) = \left[\rho_m^2 + \left(\rho_b^2 - \rho_m^2\right)\tanh^2\theta\right]^{1/2},$$
$$\phi(\xi) = -\sqrt{\frac{6|\mu|}{|\delta|}}\,\frac{v}{\rho_m}\,\tan^{-1}\left(\frac{\sqrt{\rho_b^2-\rho_m^2}}{\rho_m}\tanh\theta\right), \quad (36)$$
$$\theta = \sqrt{\frac{|\delta|}{6|\mu|}\left(\rho_b^2-\rho_m^2\right)}\,(\xi-\xi_0).$$

This solution is valid for $\gamma < 0$, when $\delta\mu < 0$, and for $\gamma > 0$, when $\delta < 0$ and $\mu > 0$.

The stability of dark solitons can be analyzed by using the modified momentum [22–24]

$$Q = \frac{i}{2}\int_{-\infty}^{\infty}(\psi\,\partial_x\psi^\star - \psi^\star\partial_x\psi)\left(1-\rho_b^2/|\psi|^2\right)dx, \quad (37)$$

where $\psi^\star$ is the complex conjugate of ψ. Parameter Q, similar to P, is the integral invariant of Eq. (4). If $dQ(v)/dv < 0$, then the dark soliton is stable, and unstable otherwise [23,24]. To calculate Q, it is not necessary to have an explicit form of the dark soliton solution. From Eq. (30), one can find that

$$Q = v\int_{y_m}^{y_b}\sqrt{\frac{1+4\mu y}{(y_a-y)[\gamma+2\delta(y+2y_b+y_a)/3]}} \times\frac{y_b-y}{y}\,dy\,. \quad (38)$$

Equations (38) and (30) provide the dependence $Q(v)$ parametrized by y_a at fixed y_b.

We calculate numerically the integral in Eq. (38). We consider a black soliton with $\rho_b = 1$, $\rho_m = 0$, and $v = 0$. Figure 10 shows the dependence of the threshold value $\mu_{\rm th}$ on δ for $\gamma = \pm 1$. Black solitons are unstable above the threshold. As seen from Fig. 10, black solitons are stable for moderate values of δ and μ, and become unstable for sufficiently large $\mu > 0$. We mention also that the instability threshold for gray solitons ($\rho_m > 0$) is usually lower than that for black solitons.

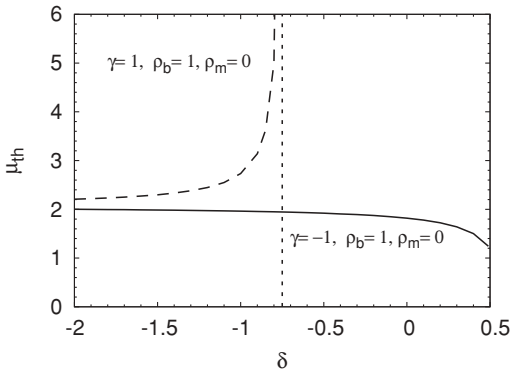

FIG. 10. Threshold value $\mu_{\rm th}$, above which black solitons with $\rho_b = 1$ and $\rho_m = 0$ are stable, as a function of δ for $\gamma = -1$ (solid line) and for $\gamma = 1$ (dashed line). For $\gamma = 1$, black solitons exist on the left-hand side from the vertical dotted line.

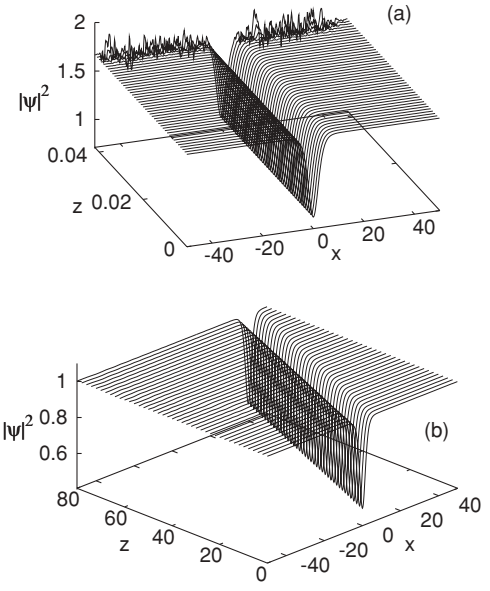

FIG. 11. Dynamics of gray solitons for $\gamma = -1$ and $\delta = 0.3$. (a) Instability of the background at $\mu = -0.3$ and $\rho_b = 1.291$. (b) Stable propagation at $\mu = -0.1$ and $\rho_b = 1$.

To study different types of the soliton dynamics, we consider the initial condition as in Ref. [24]:

$$\psi(x,0) = \left\{\rho(x) + \varepsilon\left[\rho_b^2 - \rho^2(x)\right]\right\}\exp[i\phi(x)], \quad (39)$$

where $\rho(x)$ and $\phi(x)$ are from the exact solution (36). In all of the following numerical examples, we take a gray soliton with $y_m = y_a = y_b/2$. For given δ and μ, the value of y_b is defined by Eq. (35).

First, we analyze the dynamics at $\gamma = -1$. Usually, dark solitons with the high background amplitude ρ_b are unstable. For $\delta > 0$ and $\mu < 0$, a large ρ_b for solution (36) is realized when δ is small, and/or $|\mu|$ is large. Figure 11(a) shows the soliton dynamics at $\delta = 0.3$, $\mu = -0.3$, and $\rho_b = 1.291$. One can see that the soliton background is unstable. This is a typical scenario of instability of the gray soliton (36) for such signs of δ and μ. Solitons with lower background are stable, as shown Fig. 11(b), where $\delta = 0.3$, $\mu = -0.1$, and $\rho_b = 1$. For $\delta < 0$ and $\mu > 0$, the gray soliton (36) is stable, at least when $0 > \delta > -2$ and $0.2 > \mu > 0$. It should be mentioned that for $\delta < 0$ and $\mu > 0$, the general dark soliton solution of Eq. (4) may become unstable.

Now we consider the case $\gamma = 1$, $\delta < 0$, and $\mu > 0$. Similarly to the results for black solitons (see Fig. 10), an increase of μ and/or ρ_b can induce the soliton instability. Figure 12(a) shows the development of instability for $\delta = -0.2$, $\mu = 0.8$, $\rho_b = 1.768$, and $\varepsilon = -0.005$. The gray soliton transforms initially into the black one. The latter breaks into two kinks moving in opposite directions. This dynamics is similar to what occurs in a local cubic-quintic media with $\gamma > 0$ and $\delta < 0$ [24]. The dynamics depends also on the sign of the modulation parameter ε. Figure 12(b) shows the dynamics for the same parameters as those in Fig. 12(a), but at $\varepsilon = 0.005$. Here the gray soliton transforms smoothly to that with the larger minimum amplitude. Since the variation of the amplitude is small, it is not noticeable in the figure.

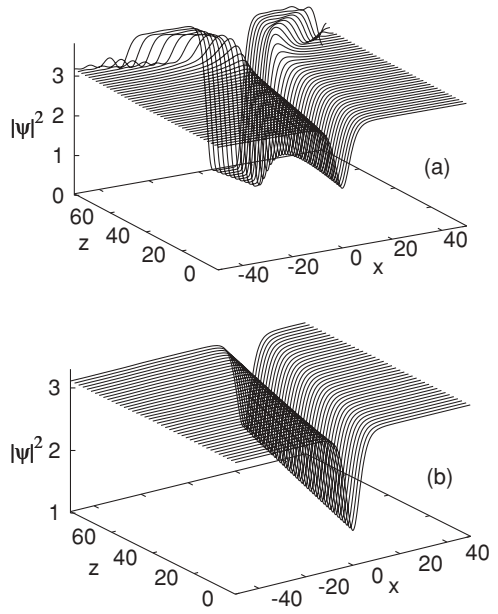

FIG. 12. Dynamics of gray solitons for $\gamma = 1$, $\delta = -0.2$, $\mu = 0.8$, and $\rho_b = 1.768$. (a) Soliton splitting into two kinks for $\varepsilon = -0.005$. (b) Transformation of the soliton into that with the larger minimum amplitude for $\varepsilon = -0.005$.

We find that results of all numerical simulations considered are consistent with the prediction of the stability condition. A dark soliton is unstable as soon as dQ/dv becomes positive.

IV. CONCLUSIONS

In the present paper, we have found exact solutions for bright and dark solitons in weakly nonlocal media with cubic-quintic nonlinearity. In general, the solutions are implicit in terms of the elliptic integrals. They can be reduced, for the particular values of the parameters, to explicit solutions in terms of the hyperbolic functions. The soliton profile can be cusp shaped, bell shaped, or flat topped, depending on the system parameters.

The stability of bright solitons has been analyzed by using the dependence of soliton power P on the propagation constant. It has been demonstrated that for $\gamma > 0$, bright solitons can be unstable, when $\mu < 0$. This is because nonlocality with negative μ increases self-focusing properties near the beam center. A typical scenario of the unstable dynamics for these parameters is the soliton collapse. It was also shown that stable bright solitons exist for defocusing cubic nonlinearity $\gamma < 0$ and $\mu > 0$, provided that the soliton amplitude is above the threshold. Solitons with the amplitude below the threshold spread, since nonlinearity cannot balance diffraction.

The regions of existence of dark solitons in weakly nonlocal media have been identified. The stability of dark solitons has been studied by using the modified momentum Q. It has been shown that black solitons are stable for the small nonlocality parameter $\mu > 0$, and become unstable when μ increases. The development of instability has been studied for gray solitons with $y_m = y_b/2$. Typical regimes of instability include the growth of perturbation on the background and the splitting of the dark soliton into two kinks.

Our study provides further insight into an interplay between competing nonlinearities and nonlocality. We demonstrate that nonlocal effects can stabilize solitons that are unstable in local media.

APPENDIX

The elliptical integrals of the first, second, and third kinds, $F(\lambda,q)$, $E(\lambda,q)$, and $\Pi(\lambda,m,q)$, respectively, are defined as follows [20]:

$$F(\lambda,q) = \int_0^{\sin\lambda} \frac{dx}{\sqrt{(1-x^2)(1-q^2x^2)}},$$
$$E(\lambda,q) = \int_0^{\sin\lambda} \frac{\sqrt{1-q^2x^2}}{\sqrt{1-x^2}}\,dx, \qquad \text{(A1)}$$
$$\Pi(\lambda,m,q) = \int_0^{\sin\lambda} \frac{dx}{(1-mx^2)\sqrt{(1-x^2)(1-q^2x^2)}}\,d.$$

[1] S. Akhmanov, D. P. Krindach, A. V. Migulin, A. P. Sukhorukov, and R. V. Khokhlov, IEEE J. Quantum Electron. **4**, 568 (1968).

[2] A. G. Litvak, V. A. Mironov, G. M. Fraiman, and A. D. Yunakovskii, Fiz. Plazmy **1**, 60 (1975) (in Russian).

[3] C. Rotschild, B. Alfassi, O. Cohen, and M. Segev, Nat. Phys. **2**, 769 (2006).

[4] M. Segev, B. Crosignani, A. Yariv, and B. Fischer, Phys. Rev. Lett. **68**, 923 (1992).

[5] S. Gatz and J. Herrmann, Opt. Lett. **23**, 1176 (1998).

[6] B. Crosignani, A. Degasperis, E. DelRe, P. Di Porto, and A. J. Agranat, Phys. Rev. Lett. **82**, 1664 (1999).

[7] E. DelRe, B. Crosignani, P. Di Porto, Prog. Opt. **53**, 153 (2009).

[8] E. Braun, L. P. Faucheux, and A. Libchaber, Phys. Rev. A **48**, 611 (1993).

[9] M. Peccianti, A. D. Rossi, G. Assanto, A. De Luca, C. Umeton, and I. C. Khoo, Appl. Phys. Lett. **77**, 7 (2000).

[10] C. Conti, M. Peccianti, and G. Assanto, Phys. Rev. Lett. **92**, 113902 (2004).

[11] P. D. Rasmussen, O. Bang, and W. Krolikowski, Phys. Rev. E **72**, 066611 (2005).

[12] A. Parola, L. Salasnich, and L. Reatto, Phys. Rev. A **57**, R3180 (1998).

[13] A. Griesmaier, J. Werner, S. Hensler, J. Stuhler, and T. Pfau, Phys. Rev. Lett. **94**, 160401 (2005).

[14] B. B. Baizakov, F. Kh. Abdullaev, B. A. Malomed, and M. Salerno, J. Phys. B: At. Mol. Opt. Phys. **42**, 175302 (2009).

[15] T. Lahaye, C. Menotti, L. Santos, M. Lewenstein, and T. Pfau, Rep. Prog. Phys. **72**, 126401 (2009).

[16] Yu. S. Kivshar and G. Agrawal, *Optical Solitons: From Fibers to Photonic Crystals* (Academic, New York, 2003).

[17] W. Krolikowski and O. Bang, Phys. Rev. E **63**, 016610 (2000).

[18] W. Krolikowski, O. Bang, N. I. Nikolov, D. Neshev, J. Wyller, J. J. Rasmussen, and D. Edmundson, J. Opt. B **6**, S288 (2004).

[19] Kh. I. Pushkarov, D. I. Pushkarov, and I. V. Tomov, Opt. Quantum Electron. **11**, 471 (1979).

[20] I. S. Gradshteyn and I. M. Ryzhik, *Table of Integrals, Series, and Products*, 4th ed. (Fizmatgiz, Moscow, 1963) (in Russian).

[21] C. De Angelis, IEEE J. Quantum Electron. **30** (No. 3), 818 (1994).

[22] Yu. S. Kivshar and W. Krolikowski, Opt. Lett. **20**, 1527 (1995).

[23] I. V. Barashenkov, Phys. Rev. Lett. **77**, 1193 (1996).

[24] D. E. Pelinovsky, Yu. S. Kivshar, and V. V. Afanasjev, Phys. Rev. E **54**, 2015 (1996).